

# Estimation of Convective Heat Transfer Coefficient and Hourly Yield of a Single Slope Solar Still: A Numerical Approach

Mojtaba Edalatpour<sup>1</sup> and Ali Kianifar<sup>2</sup>

<sup>1,2</sup>Department of Mechanical Engineering, Ferdowsi University of Mashhad, Mashhad, Iran  
E-mail: <sup>1</sup>mojtaba.edalatpour@stu.um.ac.ir, <sup>2</sup>a-kiani@um.ac.ir

---

**Abstract**—Single slope solar stills are known as popular and cheap desalination systems which have been utilized commonly all around the world to produce fresh water from salty and useless water. This paper studies natural convection heat transfer coefficient, hourly yield and fluid flow inside a single slope solar still. A finite element method is used to solve continuity, momentum, energy and concentration conservation equations. Moreover, the fluid flow within the still is considered to be incompressible, laminar, steady and ideal gas. Results are validated with several experimental investigations conducted by preceding researchers. The results also show an excellent agreement with previously published data. Furthermore, an optimum length of the still in which the productivity of the single slope solar still is maximized will be posed while the lengths of both lateral walls are constant.

## 1. INTRODUCTION

Single slope solar stills (SSSS) are considered to be one of the most consequential and well-known desalination equipment in which pure and potable water is generated from waste and saline water by solar radiation of sun. Exploiting of such facilities is simple, cheap and has low maintenance expenses in comparison with other desalination method namely reverse osmosis, vapor compression and eventually electro-dialysis processes. Utilization of these thermal systems is extremely beneficial regarding productivity and economics particularly in arid climate countries since solar radiation is abundant, free and clean [1]. Furthermore, using solar energy diminishes consumption of fossil-fuels and other detrimental pollutants. Great deals of investigations have been performed to enhance the performance of solar stills experimentally, theoretically and computationally. The vast majority of researchers concentrated on the experimental procedures to find and optimize a better design of solar stills. Voropoulos et al. [2] reported that using a solar collector can augment the productivity of a solar still by external heating of water. Partially cooled glass cover was shown to increase the performance of solar still by Zeroual et al. [3]. Phadataré and Verma's [4] research illustrated that glass covered solar still can produce 30% more output, in contrast to plastic covered solar still. In addition to experimental endeavors to raise

freshwater production, which are time consuming and costly, some researchers focused on mathematical modeling to define essential and influential parameters in solar still designing and productivity. Al-Hinai et al. [5] reported that solar radiation, wind velocity and ambient temperature play prominent roles on productivity of a solar still. Maximizing temperature differences between water and glass cover was anticipated to enhance the production of freshwater within the basin by Abdenacer and Nafila [6]. Kianifar and Mahian [7] conducted an investigation through using a low-powered fan inside a solar still. Their results depicted that using a fan results in potable water production improvement.

Moreover, multiplicity of researches have been carried out based on computational fluid dynamics (CFD) since CFD declines substantially cost, time and also some major parameters namely ambient temperatures and configurations can be altered simply, as well. Setoodeh et al. [8] exploited computational fluid dynamics methods and reported that the amount of fresh water productivity and water temperature were in good agreement with benchmark experimental data. Moreover, they concluded that CFD is a tremendous tool for design, parameter analyses and diagnostic purposes of solar still. Rahman et al. [9] modeled double-diffusive natural convection inside a triangular solar collector using finite element method. Their research demonstrated that increasing in buoyancy ratio results in increasing the heat transfer rate and as a consequent productivity of solar still improves. The designing procedure of solar still to pinpoint its optimized value which has the highest amount of water productivity is conducted in this paper. As it was mentioned above, due to expensive experimental construction of such facilities and time consuming processes, computational fluid dynamics is exploited in this area. No sufficient studies on the CFD optimization of solar stills have been conducted to the best knowledge of the authors of this research paper. Therefore, the aim of this study is to use a numerical approach for studying the fluid flow, local and average Nusselt number and assessment of hourly-yield of a single slope solar still. In any

case, the ability of implementation of CFD in the field of solar still optimization is investigated, as well.

**2. THEORETICAL BACKGROUND**

The convective heat transfer occurs in the form of double-diffusive natural convection within the solar still. Natural convection inside the solar still takes place due to the buoyant forces generated by density variation because of both temperature and concentration gradients simultaneously. In the following, several thermal models exploited to study such phenomenon will be presented.

**2.1 Thermal models**

The rate of heat transfer between the water and glass cover can be expressed as [10]:

$$q_c = h_c A (T_w - T_g) \tag{1}$$

The convective heat transfer coefficient,  $h_c$ , is the function of fluid properties, operating conditions and flow characteristics. Various experimental models were propounded to assess the internal heat transfer coefficient inside the still given as follows:

**2.1.1 Dunkle model**

The widely used equation to estimate the heat transfer coefficient was given by Dunkle [11], initially.

$$h_c = 0.884(\Delta T')^{1/3} \tag{2}$$

where

$$\Delta T' = \left[ (T_w - T_g) + \frac{(P_w - P_g)(T_w + 273)}{268.9 \times 10^3 - P_w} \right] \tag{3}$$

$$P_w = \exp\left(25.317 - \frac{5144}{T_w + 273}\right) \tag{4}$$

$$P_g = \exp\left(25.317 - \frac{5144}{T_g + 273}\right) \tag{5}$$

Another form of Dunkle model is:

$$Nu = 0.075(Ra')^{1/3} \tag{6}$$

where

$$Ra' = \frac{\rho^2 g \beta c_p H^3 \Delta T}{\mu k} \tag{7}$$

**2.1.2 Shawaqfeh and Farid model**

Another experimental study was conducted by Shawaqfeh and Farid [12] based on Bulk motion and Chilton-Colburn analogies. Furthermore, they reported that Dunkle model

overpredicts the convective heat transfer coefficient inside the still by about 30%, as well.

$$Nu_{BM} = 0.057(Ra')^{1/3} \tag{8}$$

$$Nu_{CC} = 0.057(Ra')^{1/3} \tag{9}$$

**2.1.3 Corcione model**

Corcione [13] proposed an equation based on numerical analysis for multiplicity of aspect ratio to evaluate the convective heat transfer inside the still.

$$Nu = 0.21 \left(\frac{L}{H}\right)^{0.09} Ra^{0.25} \tag{10}$$

where  $Ra$  can be calculated as similar as that in Eq. (7). In all of the above equations, the properties of humid air are estimated by calculation of mean temperature between water and glass cover temperatures  $T = (T_w + T_g)/2$ .

**3. PROBLEM STATEMENT**

**3.1 Physical description**

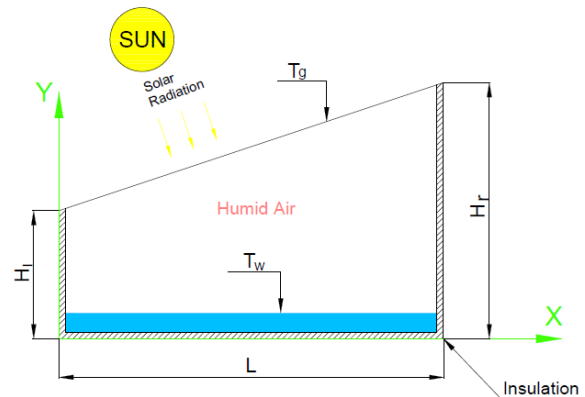


**Fig.1: A schematic view of the solar still**

The geometry for configuration of discussed problem is shown by a schematic diagram in Fig. 1. The model deemed here is a single slope solar still. The enclosed space is comprised of two lateral walls which are assumed to be adiabatic and impermeable, whereas water and glass surfaces are imposed to constant temperatures of  $T_w$  and  $T_g$ , respectively.

**3.2 Mathematical formulation**

The salty water on the bottom surface of the enclosure is vaporized. The vapor moves through air and condenses at the glass cover since  $T_w > T_g$ . The fluid flow is considered to be as steady-state, humid air, incompressible ideal gas with constant physical properties and negligible viscous dissipation. Due to low operating temperatures, radiation mode is assumed to be negligible.

By the aforesaid assumptions, the governing equations which represented of conservation equations of mass, momentum, energy and concentration, in dimensionless Cartesian form are as follows [14]:

Continuity:  

$$U \frac{\partial U}{\partial X} + V \frac{\partial V}{\partial Y} = 0$$
 10

X-Momentum:  

$$U \frac{\partial U}{\partial X} + V \frac{\partial U}{\partial Y} = -\frac{\partial P}{\partial X} + Pr \left( \frac{\partial^2 U}{\partial X^2} + \frac{\partial^2 U}{\partial Y^2} \right)$$
 11

Y-Momentum:  

$$U \frac{\partial V}{\partial X} + V \frac{\partial V}{\partial Y} = -\frac{\partial P}{\partial Y} + Pr \left( \frac{\partial^2 V}{\partial X^2} + \frac{\partial^2 V}{\partial Y^2} \right) + RaPr (\theta - BrC)$$
 12

Energy:  

$$U \frac{\partial \theta}{\partial X} + V \frac{\partial \theta}{\partial Y} = \frac{\partial^2 \theta}{\partial X^2} + \frac{\partial^2 \theta}{\partial Y^2}$$
 13

Diffusion:  

$$U \frac{\partial C}{\partial X} + V \frac{\partial C}{\partial Y} = \frac{1}{Le} \left( \frac{\partial^2 C}{\partial X^2} + \frac{\partial^2 C}{\partial Y^2} \right)$$
 14

The boundary conditions are:

at top :  $U = 0, V = 0, \theta = 0, C = 0$

at bottom :  $U = 1, V = 1, \theta = 1, C = 1$  15

at lateral walls:  $U = 1, V = 1, \theta/\partial X = 1, C/\partial X = 1$

**4. SOLUTION PROCEDURE**

The system of governing equations, Eqs. (10)-(14), were solved by the control volume method using FLUENT software. Discretization of convection terms, diffusion terms, and other quantities resulting from governing equations was carried out using second-order upwind. The pressure-velocity coupling was modelled with the SIMPLEC algorithm (semi implicit method for pressure linked equations consisted) described by Patankar [15]. Then, the solution was deemed to be fully converged since the values of scale-residuals were smaller than  $10^{-3}$ , except for energy equation,  $10^{-6}$ . After the convergence was attained, the average Nusselt number,  $\overline{Nu}$ , and the hourly-yield were calculated by given formulas:

$$\overline{Nu} = \int_0^1 \frac{\partial \theta}{\partial n} \Big|_{water} dX$$
 16

$$\dot{m}_{hourly} = \frac{-3600 \times D_{AB}}{L} \int_0^L \frac{\partial C}{\partial n} \Big|_{water} dx$$
 17

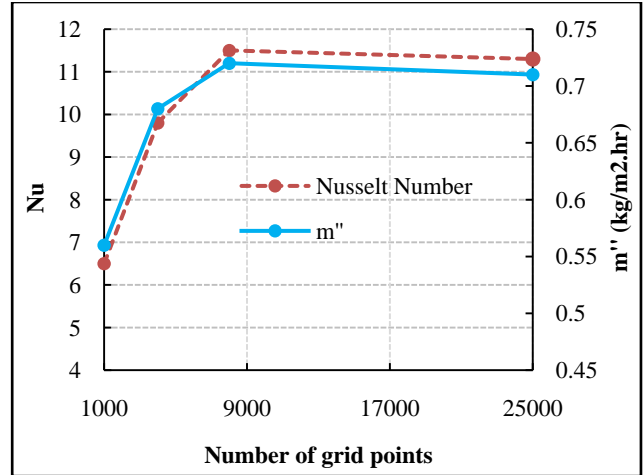


Fig. 2: Grid-dependency check for a single slope solar still, case 1 in table 2

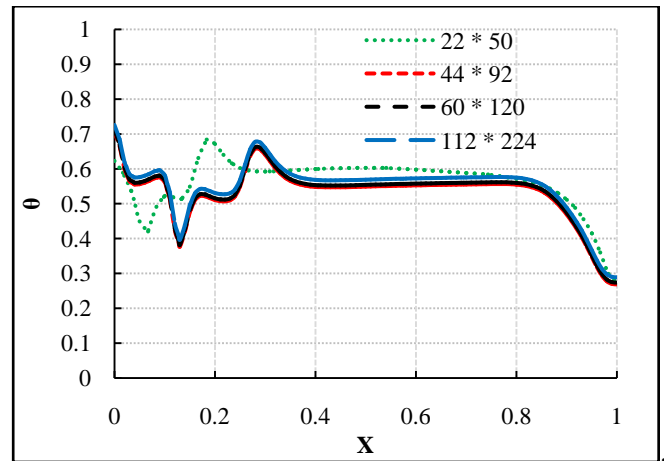


Fig.3: Comparison of temperature profiles at mid-section of the still.

Calculation of temperature and concentration integrals was performed exploiting compound trapezoid computing rule. To measure and assess grid-dependency test, an extensive mesh testing was conducted for all the investigated configurations in this paper to assure a grid independent solution. 4 different non-uniform mesh combinations were used for the case No. 1 in table 1.

Table 1: Geometry of set-up solar stills by previous researchers and thermal conditions [12, 16].

Case No.	$T_w$	$T_g$	$H_r$	$H_l$	$L$	inclination angle
1	63	48	0.187	0.075	0.438	14.35°
2	50	40	0.1	0.47	0.98	19°
3	70	60	0.1	0.47	0.98	19°

Evaluation of grid independency test was used by calculating the average Nusselt number and productivity within the solar still illustrated in Fig.2. It is found that a grid size  $60 \times 120$  ensures a grid independent solution. Furthermore, a comparison between four aforementioned meshes in terms of dimensionless temperature in the middle section of the still was carried out and its results are depicted in Fig. 3. As it is clear, grid mesh  $60 \times 120$  is sufficient to describe the fluid flow, heat and mass transfer phenomena within the enclosure. Further increment in the number of grid points produces the same results, with respect to the featured figures.

**4.2 Validation**

In order to validate the present numerical code, the solution was compared with the experimental data for two different solar still geometries reported by Tiwari et al. [16] and Shawaqfeh and Farid [12] tabulated in table 2.

**Table 2: Comparison between CFD code and experimental data reported by previous researchers [12, 16].**

	Present code	Dunkle model	Chilton-Colburn Model	Bulk motion Model
Case No. 1				
$\overline{Nu}$	11.1	12.1	8.23	9.2
$\dot{m}_{hourly}$	18.9	21	N.A	N.A
Case No. 2				
$\overline{Nu}$	15.65	22.3	15.2	17.0
$\dot{m}_{hourly}$	5.19	7.11	4.79	5.98
Case No. 3				
$\overline{Nu}$	16.3	23.8	16.2	18.0
$\dot{m}_{hourly}$	14.56	18.8	14	18.4

**5. RESULTS AND DISCUSSIONS**

Fig. 4 and 5 denote streamlines and isotherms of a single slope solar still. The bottom and glass cover temperatures of Fig.4 and 5 are constant and  $313K$  and  $303K$ , respectively. As it can be seen in these figures, 3 circulation cells (vortexes), and 2 thermal plumes; downward and upward, exist within the single slope solar still. The middle one rotates clockwise, whereas the other vortexes near the lateral walls rotate counterclockwise. To put it differently, humid air moves from the glass cover to the bottom wall by the middle vortex, while for the circulation cells near the sides of the solar still, they ascend from the bottom wall to the glass cover.

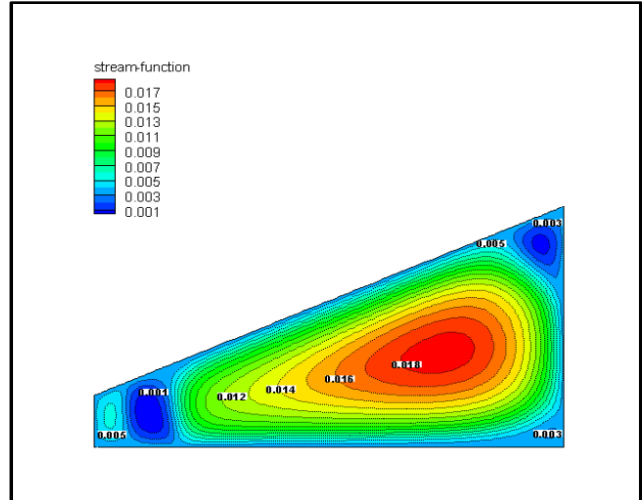


**Fig.4: Streamlines for  $Ra=10^4$ , case 2 in table 1.**

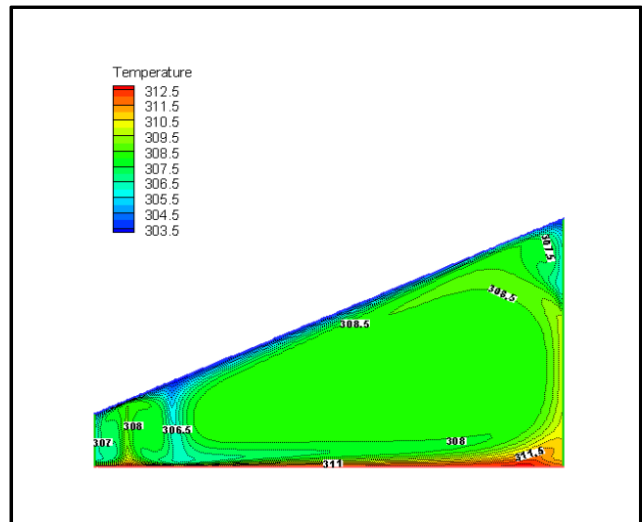


**Fig.5: Isotherms for  $Ra=10^4$ , case 2 in table 1.**

Fig. 6 depicts CFD estimation of Nusselt number and water productivity of a single slope solar still, case 2 in table 1, for multiplicity of still lengths. As it can be observed from the figure, the trend of the Nusselt number is similar to the trend of hourly yield within the solar still.

Additionally, in the range of  $0.3 < L < 1.0$ , there is an optimum length in which the hourly yield is maximized. The optimum length and maximum water productivity are  $L = 0.75m$  and  $\dot{m}'' = 0.865 \text{ kg}\cdot\text{m}^{-2}\cdot\text{hr}^{-1}$ , respectively.

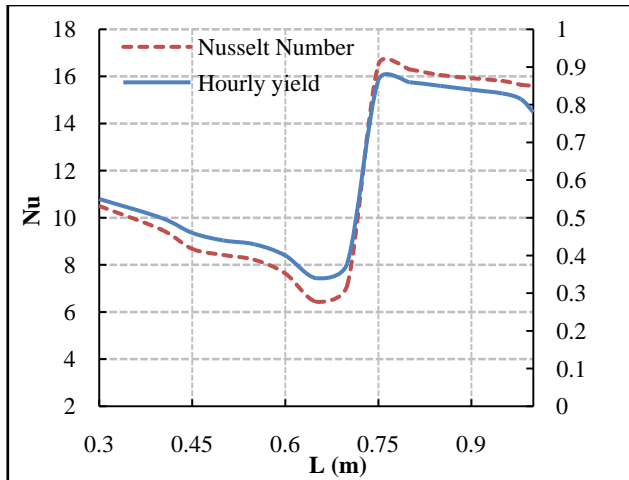


Fig. 6: Variation of Nusselt number and hourly yield vs. various length of still, case 2 in table 1.

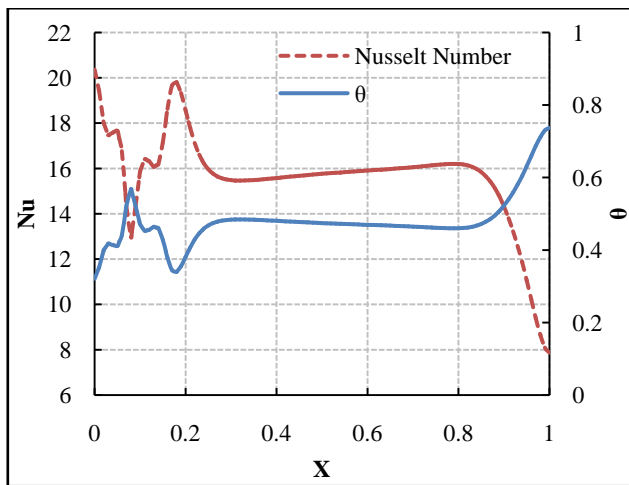


Fig. 7: Variation of dimensionless temperature and Nusselt number inside the solar still, ( $L = 0.75, Ra = 2.1 \times 10^5$ ).

Fig.7 shows the fluctuation of the dimensionless temperature,  $\theta = (T - T_c)/(T_h - T_c)$ , and the local Nusselt number inside the single slope solar still. As it can be seen evidently, there are two plumes within the still; downward and upward. The minimum local Nusselt number occurs in the area where flow directed upward from water surface to glass cover at  $X = 0.08$ , while the maximum local Nusselt number is in the region where flow directed downward from glass cover to water surface at  $X = 0.18$ . Therefore, the more downward plumes exist inside the still, the more convective heat transfer will be.

Fig. 8 shows the fluctuation of dimensionless vertical velocity,  $V = vL/\alpha$ , and the local Nusselt number. It can be concluded that the trend of vertical velocity and temperature are always as similar to each other within the solar still in reference to Fig.7 and 8. The Nusselt number declines in the

region where humid air moves upward, while it is increased by downward movement of fluid flow.

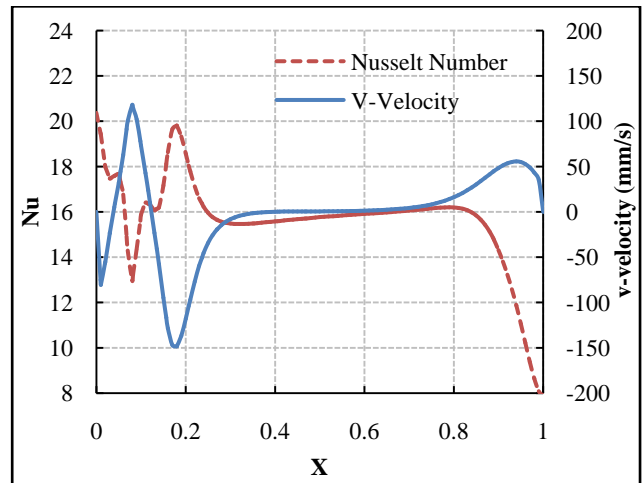


Fig. 8: Variation of v-velocity and Nusselt number inside the solar still, ( $L = 0.75, Ra = 2.1 \times 10^5$ ).

## 6. CONCLUSION

A numerical code has been developed to study the fluid flow, convective heat and mass transfer inside the single slope solar still. The principal points of this paper are as follows:

1. CFD is a powerful tool to investigate the natural convection heat transfer and hourly yield of single slope solar still.
2. There is an optimum still length, in which the freshwater productivity is maximized.
3. The more downward plumes are inside the still, the better productivity will be as a result of increment in natural convection heat transfer.
4. The air moves upward in the area where flow directed upward, while it moves downward in the area where flow directed downward.
5. The trend of heat and mass transfer within the still is always similar to each other.
6. The trend of temperature and local Nusselt number is opposite to each other.

## 7. NOMENCLATURE

Br	buoyancy ratio
C	dimensionless species concentration
$C_p$	specific heat $\text{kJ.kg}^{-1}.\text{k}^{-1}$
D	mass diffusivity of vapor $\text{m}^2.\text{s}^{-1}$
g	gravitational acceleration $\text{m.s}^{-2}$
$H_l$	height of the left side of solar still <b>m</b>
$H_r$	height of the right side of solar still <b>m</b>
h	heat transfer coefficient $\text{W.m}^{-2}.\text{k}^{-1}$

k	thermal conductivity $\text{W}\cdot\text{m}^{-1}\cdot\text{K}$
L	length of solar still $\text{m}$
Le	Lewis number
Nu	Nusselt number
p	dimensional pressure $\text{Pa}$
P	non-dimensional pressure
q	rate of heat transfer
Pr	Prandtl number
Ra	Rayleigh number
T	dimensional temperature $^{\circ}\text{C}$
$\Delta T$	temperature difference between water and glass $^{\circ}\text{C}$
u	horizontal velocity component $\text{m}\cdot\text{s}^{-1}$
U	dimensionless horizontal velocity component
v	vertical velocity component $\text{m}\cdot\text{s}^{-1}$
V	dimensionless vertical velocity component
x	horizontal coordinate $\text{m}$
X	dimensionless horizontal coordinate
y	vertical coordinate $\text{m}$
Y	dimensionless vertical coordinate
$\alpha$	thermal diffusivity $\text{m}^2\cdot\text{s}^{-1}$
$\beta$	thermal expansion coefficient $\text{K}^{-1}$
$\theta$	non-dimensional temperature
$\mu$	viscosity $\text{N}\cdot\text{s}\cdot\text{m}^{-2}$
$\rho$	density $\text{kg}\cdot\text{m}^{-3}$
c	convective
g	glass
n	normal direction to the surface
w	water surface

## REFERENCES

- [1] Kaushal, A., Varun, "Solar stills: a review". *Renewable and Sustainable Energy Reviews*, 14, 1, January 2010, pp. 446-453.
- [2] Voropoulos, K., Mathioulakis, E., Belessiotis, V., "Experimental investigation of a solar still coupled with solar collectors", *Desalination*, 138, September 2001, pp. 103-110.
- [3] Zeroual, M., Bouguettaia, H., Bechki, D., Boughali, S., Bouchekima, B., Mahcene, H., "Experimental investigation on a double-slope solar still with partially cooled condenser in the region of Ouargla (Algeria)", *Energy Procedia*, 6, 7, 2011, pp. 736-742.
- [4] Phadatare, M.K., Verma, S.K., "Influence of water depth on internal heat and mass transfer in a plastic solar still", *Desalination*, 217, November, 2007, pp. 267-275.
- [5] Al-Hinai, H., Al-Nassri, M.S., Jubran, B.A., "Effect of climatic, design and operational parameters on the yield of a simple solar still", *Energy Conversion and Management*, 43, 13, September 2002, pp. 1639-1650.
- [6] Abdenacer, P.K., Nafila, S., "Impact of temperature difference (water-solar collector) on solar-still global efficiency". *Desalination*, 209, April 2007, pp. 298-305.
- [7] Mahian, O., Kianifar, A., "Mathematical modelling and experimental study of a solar distillation system". *Part C: Journal of Mechanical Engineering Science*, 225, 3, May 2011, pp. 1203-1212.
- [8] Setoodeh, N., Rahimi, R., Ameri, A., "Modeling and determination of heat transfer coefficient in a basin solar still using CFD", *Desalination*, 268, March 2011, pp. 103-110.
- [9] Rahman, M.M., Öztop, H.F., Ahsan, A., Kalam, M.A., Varol, Y. "Double-diffusive natural convection in a triangular solar collector", *International Communication in Heat and Mass Transfer*, 39, 2, February 2012, pp. 264-269.
- [10] Sampathkumar, K., Arjunan, T.V., Pitchandi, P., Senthilkumar, P., "Active solar distillation a detailed review", *Renewable and Sustainable Energy Reviews*, 14, 6, August 2010, pp. 1503-1526.
- [11] Dunkle, R., "Solar water distillation; the roof type still and a multiple effect-diffusion still, internet", *International Developments in heat transfer, ASME*, 1961.
- [12] Shawaqfeh. A.T., Farid, M.M., "New development in the theory of heat and mass transfer in solar stills", *Solar Energy*, 55, 6, 1995, pp. 527-535.
- [13] Corcione, M., "Effects of the thermal boundary conditions at the sidewalls upon natural convection in rectangular enclosures heated from below and cooled from above", *International Journal of Thermal Science*, 42, 2, February 2003, pp. 199-208.
- [14] Talukdar, P., Iskra, C.R., Simonson, C.J., "Combined heat and mass transfer for laminar flow of moist air in a 3D rectangular duct: CFD simulation and validation with experimental data", *International Journal of Heat and Mass Transfer*, 51, June 2008, pp. 3091-3102.
- [15] Patankar, S.V., *Numerical heat transfer and fluid flow*, Hemisphere, 1980.
- [16] Tiwari, G.N., Minocha, A., Sharma, P.B., Emran Khan, M., "Simulation of convective mass transfer in a solar distillation process", *Energy Conversion and Management*, 38, 8, May 1997, pp. 761-770.